PHYSICAL REVIEW B VOLUME 16, NUMBER 4 15 AUGUST 1977

Transport and recombination in sputtered hydrogenated amorphous germanium*

T. D. Moustakas† and William Paul
Division of Engineering and Applied Physics, Harvard University, Cambridge, Massachusetts 02138
(Received 24 March 1977)

The steady-state and transient photoconductivity of sputtered hydrogenated amorphous Ge (T_s = 300 K) was studied as a function of wavelength, light intensity, and temperature. The reduction of low-temperature dark conductivity and the shift to higher energies of the photoconductivity edge with hydrogenation are consistent with the notion that hydrogen eliminates states from the pseudogap. The magnitude and the temperature dependence of the drift mobility between 77 and 300 K was inferred from the measurements. Above about 200 K the mobility had an activation energy of 0.1 eV, while below 200 K it was only weakly T dependent. This variation with T is theoretically predicted from small-polaron theory, viz., hopping with an activation energy of half the polaron binding energy above $T_0 = \hbar\omega_0/2k$, where $\hbar\omega_0$ is the optical phonon energy, and hopping at low T with an activation energy equal to the disorder energy. From these data the disorder energy is estimated to be of the order of 0.01 eV. To account for a weak dependence of the lifetime on temperature and on hydrogenation, we propose a model in which the photocarriers form small polarons which degrade in energy while they are moving in the applied field.

I. INTRODUCTION

Transport in amorphous Ge thin films[1] is generally supposed to proceed by two qualitatively different mechanisms: the first, which is dominant at relatively high temperatures, involves the motion of conduction-band electrons and valence-band holes among the states intrinsic to the completely coordinated, but disordered, network; the second, which is dominant at low temperatures, involves the transport (by tunneling or hopping or both) of carriers between extrinsic states with energies in the pseudogap. Understanding of the origin and properties of these extrinsic states is essential to the establishment of an adequate description of the semiconductor. Structural measurements[2] have shown that sputtered films contain a distribution of voids of the order of 5–10-Å diameter. Optical, transport, and electron-spin-resonance measurements[3,4] have been plausibly and self-consistently interpreted on a model which identifies the majority of pseudogap electrons with those on these internal void surfaces.

Deposition or annealing at high temperatures[4] decreases the low-temperature conductivity, which is consistent with a reduction in the pseudogap state density and an observed decrease in the void volume. Controlled addition of hydrogen to the sputtering gas[5,6] produces profound systematic changes in properties, which are easily understood on the supposition that the hydrogen forms a strong bond with Ge atoms on void surfaces, and thereby eliminates states from the pseudogap.

Lewis[5] has made an extensive study of the conductivity and thermoelectric power as a function of temperature for samples of different hydrogen content prepared in this laboratory by rf sputtering. As the amount of incorporated hydrogen is increased, the high-temperature bandlike activated conductivity extends to lower temperatures consistent with a decrease in transport through pseudogap states. He finds a difference of approximately 0.2 eV between the activation energy for band conductivity and the slope of thermoelectric power versus reciprocal temperature. He correlated this with other observations and suggested that high-temperature transport occurs by small-polaron hopping. According to small-polaron theory[7-10] the hopping energy should decrease considerably near $\frac{1}{2}\Theta - \frac{1}{4}\Theta$, where Θ is the characteristic temperature of the optical phonons $\hbar\omega_0/k$. In a-Ge, $\hbar\omega_0 \approx 0.035$ eV,[6] and the predicted decrease in activation energy occurs for temperatures less than $\frac{1}{2}\Theta$ or 200 K. However, Lewis finds that below approximately 200 K, transport near the Fermi level, in the pseudogap, dominates the band conduction, and thus prevents verification of this aspect of the hypothesized small-polaron conduction.

Photoconductivity studies on a-Ge are rather scarce,[11-15] presumably because of the low photoresponse. Care must be taken to correct for or eliminate bolometric effects due to the illumination, which may in fact be the dominant effect under some experimental conditions. The photoconductivity depends *inter alia* on the product of the mobility μ and the recombination lifetime τ. Unless independent measurements of μ or τ are made, the same set of photoconductivity data may be interpreted in different ways, depending on the postulated mechanisms for μ or τ.

In this paper, we report steady-state and transient-photoconductivity studies on a series of amorphous-Ge thin films with different hydrogen concentrations. The photoconductivity was studied

as a function of photon energy, light intensity, and temperature. The temperature dependence of the lifetime was used to test different models proposed for the mechanism of carrier recombination. The magnitude and temperature dependence of the mobility between 77 and 300 K was inferred from that of the lifetime, and thus the predictions of the theory of small polaron formation were tested; in particular, the disappearance of the activation energy for small polarons below $\frac{1}{2}\Theta$ was examined.

In view of the dramatic effects of hydrogen addition on the pseudogap state density, another objective of this study was the investigation of the influence of hydrogen on the recombination. Hydrogen incorporation into the material could influence the recombination rate in different ways, which are not mutually exclusive. (i) For example, if the photocarriers conduct in band states and the gap states act as recombination centers, one would expect that the removal of gap states could cause a decrease in the recombination rate and an increase in the photoconductivity. (ii) On the other hand, if the carrier energy $|E-E_F|$ is dissipated by a multiphonon process near the site providing the final state for the carrier near E_F, the probability for the transition is given by $P \sim \exp(-|E-E_F|/\hbar\omega_{max})$, where $\hbar\omega_{max}$ is the maximum phonon energy. Hydrogen could accelerate this recombination by providing local modes of high energy (0.23 eV).[6] (iii) If the photocarriers thermalize rapidly down to the equilibrium Fermi level where they conduct by hopping, as suggested by Fischer and Vornholz,[12] the reduction of pseudogap state density by hydrogen incorporation could decrease the carrier mobility and increase the recombination lifetime. (iv) For our most hydrogenated samples the amount of incorporated hydrogen is estimated to be 12 at.%. Such samples might more properly be designated as germanium-hydrogen alloys, and then the possibility of changes in the valence- and conduction-band densities of states needs to be examined. The energies of the Ge-H bonding states produced by H adsorbed on a crystalline Ge surface have been determined both theoretically and experimentally, and it appears that these are roughly 5 eV below the top of the crystalline valence band.[16] It seems most plausible that H incorporated in erstwhile dangling bonds in a-Ge gives bonding states with about the same energy. Thus, although the overall valence-band density of states had undoubtedly been altered by a 12-at.% H addition, the band structure near the top of the valence band and penetrating into the pseudogap is unlikely to be affected by these Ge-H bonding-state eigenvalues. One must then examine the possibility of Ge-H antibonding-state energies. These have not been determined experimentally or theoretically. On the other hand, it is known that the bonding-antibonding state energy separation in GeH_4 and similar molecules is of the order of 7 eV,[17] suggesting that, in our problem, such states exist, suitably broadened, about 1 eV above the bottom of the conduction band. (In the case of silicon, the antibonding Si-H state would appear to land about the energy of the bottom of the a-Si conduction band. We believe that this may have serious implications for all optical and transport measurements in a-Si which contain H—an especially real possibility when this material is made from silane, SiH_4—and that the question of alteration of the conduction-band density of states, and the effect of having a different kind of eigenstate, must be seriously considered in analysis of results for this material.) While the broadening may be insufficient to cause problems at low-H concentrations, there exists the possibility that the nature and density of the states near the extremum of the conduction band is different in a 12-at.% alloy than in the pure matrix. In the event that the antibonding states have energies in the pseudogap, very severe effects must ensue for all transport and phototransport. In any event, the possible effect of the Ge-H antibonding states has to be carefully watched for in analysis of all samples, and especially in analysis of those with high atomic percentages of H.

II. EXPERIMENTAL METHODS

A. Sample preparation and characterization

Amorphous $Ge_{1-x}H_x$ films were deposited by rf sputtering (apparatus: Vacuum Industries 2305 Diode Sputtering System) of an "optical grade" polycrystalline Ge target of 5 in. diameter, at a rate of about 3 Å/sec in an argon atmosphere of 5×10^{-3} Torr. The system was first dry pumped to a base pressure of 5×10^{-7} Torr. The argon gas was of 99.9995-at.% nominal purity. Hydrogen incorporation into the films was achieved by adding hydrogen at a certain partial pressure into the sputtering gas. The hydrogen gas was of 99.999-at.% nominal purity. Four types of samples were prepared at hydrogen partial pressures of 0, 2.8×10^{-4}, 5.3×10^{-4}, and 1×10^{-3} Torr (all gauge readings were corrected by gas-sensitivity factors). The substrates, sapphire or Corning glass 7059, were ultrasonically precleaned and plasma etched at 500 V and 50 W *in situ* and kept at room temperature during the deposition. The target also was plasma etched at 250 W before each run began. A more detailed description of sample preparation is given elsewhere.[6] The concentration of impurities in the thin films has not been directly determined, but may be plausibly inferred

from earlier preparations of thick samples by rf sputtering in this laboratory. Thus the argon content may be as much as 5 at.%, and it is guessed from a qualitative correlation of argon content and void volume as a function of deposition temperature that the argon atoms may inhabit the "voids."[4] The concentration of unwanted impurities has been determined by a mass spectrometer investigation of material sputtered off films prepared in a similar apparatus[4] and found to be below 0.01 at.% for preparation conditions involving apparatus vacuums of the order of 5×10^{-6} Torr.

The present samples are of an open-cell geometry made by depositing approximately 1 μm of the active material on pre-evaporated nichrome electrodes spaced 100 μm apart. The width of the electrodes is 1.6 mm. Nichrome has been found to give Ohmic contacts to amorphous Ge.[18] The hydrogen incorporated into the samples was not directly measured because of the thinness of the films, but was estimated on the basis of a model put forward by Connell and Pawlik[6] for the mechnism of hydrogen incorporation. Lewis *et al.*[19] had attributed infrared-absorption doublets near 0.07 and 0.23 eV to bending and stretching vibrations of H in Ge-H bonds that could be in two different sites. Connell and Pawlik advanced a specific model in which the H could bond to Ge either on a void surface or in the bulk matrix. The magnitudes of the separate components of either doublet were then correlated with the partial pressure of hydrogen in the sputtering gas, and, using comparable data on absorption by GeH_4 and $GeHBr_3$ molecules, to estimate the at.%-H incorporation. Thus, they were able to estimate total hydrogen incorporations up to 9 at.% in their thick films by direct measurement of the integrated absorption. We have assumed that the thin films of the present investigation contain the same fraction of hydrogen as the earlier thick films prepared under identical conditions, and that, furthermore, the Connell and Pawlik analysis correlating the hydrogen content with the partial pressure of hydrogen in the sputtering gas may be used to estimate the hydrogen content of thin films with more than 9-at.%-H. [For a discussion of the possible errors of these estimates, the reader is referred to Connell and Pawlik, Ref. 6, Eqs. (4) and (5).] Thus, we estimate for our four types of sample that the atomic percentages of hydrogen on void surfaces and in the bulk of the films are (0, 0), (2.3, 1.8), (3, 4.4), and (3.4, 9.5). To identify these films, we will use, as in previous papers,[5,6] the notation $F(N)$ where N is the *total* at.% H bonded on void surfaces and in the bulk of the films. Thus, we have $N = 0$, 4.1, 7.4, and 12.9.

The thicknesses of the films were determined, using a Sloan Dectak thickness monitor, to be $F(0) = 0.68$ μm; $F(4.1) = 1.2$ μm; $F(7.4) = 1.05$ μm; and $F(12,9) = 1.1$ μm.

B. Photoconductivity measurements

The conductance Σ and change of conductance upon illumination $\Delta\Sigma$ were measured. Excitation sources included a 250-W quartz iodine tungsten lamp, whose light was dispersed through a monochromator (resolution 0.02 eV), a 0.5-mW He-Ne laser ($h\nu = 1.96$ eV) and a GaAs laser (LD 24 of Laser Diode Laboratories) operating at 77 K ($h\nu = 1.47$ eV). The light from the first two sources was modulated mechanically (chopping frequency: 600 Hz). These light sources were used to measure the steady-state photoconductivity. The GaAs laser was modulated electrically to produce pulses of approximately 3 μsec duration with rise and fall times of less than 100 nsec at a repetition rate of 500 Hz. This source was used for both steady-state and transient measurements. The light intensity of the He-Ne and GaAs lasers was measured with a calibrated Si detector (PIN-10 of United Detector Technology), positioned in the place of the sample and covered with an aperture having the dimensions of the sample. The spectrum of the tungsten lamp was determined with the Perkin-Elmer/1368 thermopile. Calibrated neutral density filters were used to alter the light intensity.

The photoconductance $\Delta\Sigma$ was measured by placing a battery, sample and resistor in series, and measuring the ac component of voltage across the resistor with a phase sensitive detector. The applied electric field was kept below 10^3 V/cm. The photoconductance was found to depend linearly on the applied voltage (field strength between 10 and 10^4 V/cm) for all investigated photon energies and temperatures. In the case of transient measurements, the load resistance was such that the response of the measuring system, about 100 nsec, was much faster than the signal decays under study. The signal was amplified by means of a Keithley Model 107 pulse amplifier and observed directly on an oscilloscope.

Care was taken to eliminate any possible bolometric component from the photoresponse by choosing the film conductance Σ, and the chopping frequency f such that[20]

$$\Delta\Sigma_{\text{bol}} \sim \Sigma(\tau^{-2} + 4\pi^2 f^2)^{-1/2}$$

was much smaller than the measured photoresponse. Here, τ is the thermal time constant of the device. (Thin films were selected for this study so that the resistance would be large.) In addition, the photoresponse was found to be in-

dependent of whether the substrate material was sapphire or glass. The thermal time constant of a-Ge sputtered on these substrates is known[20] to be approximately 1 and 10 msec, respectively. The fact that the measured change in conductance on illumination of the present films was found to be independent of substrate material rules out any bolometric contribution.

III. EXPERIMENTAL RESULTS

A. Dark conductivity

The dark conductivity of the amorphous Ge films investigated is shown in Fig. 1, plotted against $1/T$. It is seen that hydrogenation reduces the low-temperature conductivity by several orders of magnitude. As a result the bandlike conduction, in which the conductivity is thermally activated, extends to lower temperatures with increased hydrogenation. For example, for the most hydrogenated film, $F(12.9)$, the conductivity is thermally activated above 200 K and has the form $\sigma = 32e^{-0.33/kT}\ \Omega^{-1}\,\mathrm{cm}^{-1}$. These measurements were found to be consistent with the Lewis[5] four-probe conductivity data on thicker films prepared under the same conditions.

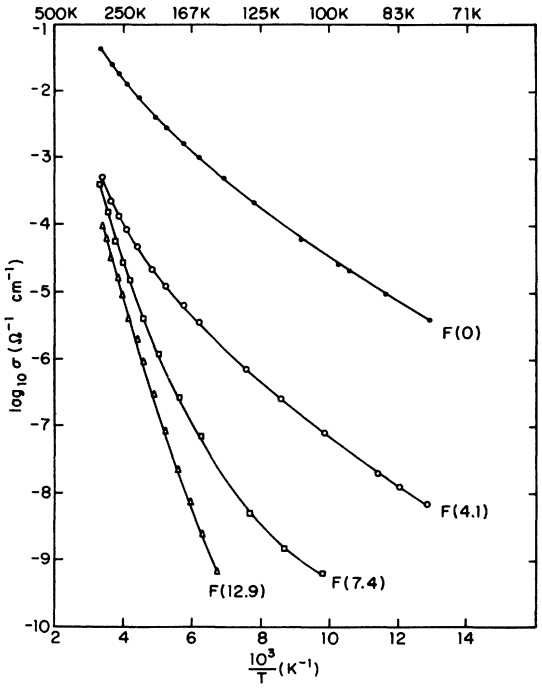

FIG. 1. Dark conductivity vs reciprocal temperature of a-Ge films deposited at different partial pressures of hydrogen. The amount of incorporated hydrogen $F(N)$ was calculated as explained in the text.

B. Photoconductivity

1. Spectral dependence

The photoconductance per incident photon $\Delta\Sigma$ is shown in Fig. 2 as a function of photon energy, with the data normalized to unity at 1.7 eV. The normalization was carried out under the assumption that the transport and recombination mechanisms are the same for all films. These spectra were measured at 77 K, except for the sample $F(4.1)$, which was measured at 117 K. The weak structure on the rapidly rising edge of the $F(0)$ sample has its origin in interference fringes. However, the minimum at 1.35 eV appears to be a property of the material, since its position is independent of sample thickness and degree of hydrogenation.

Hydrogenation shifts the normalized edge to higher energies by approximately 0.5 eV. The observed shifts are in agreement with optical absorption shifts, measured by Connell and Pawlik[6] on similar thick films.

2. Light-intensity dependence

The dependence of the photoconductance on light intensity was measured with the He-Ne laser. The photoconductance of the different samples versus light intensity at $T = 298$ and 77 K is shown in Fig. 3. For the hydrogenated films the photoconductivity depends linearly on light intensity at room temperature and becomes slightly sublinear at lower temperatures with a power between 0.92 to

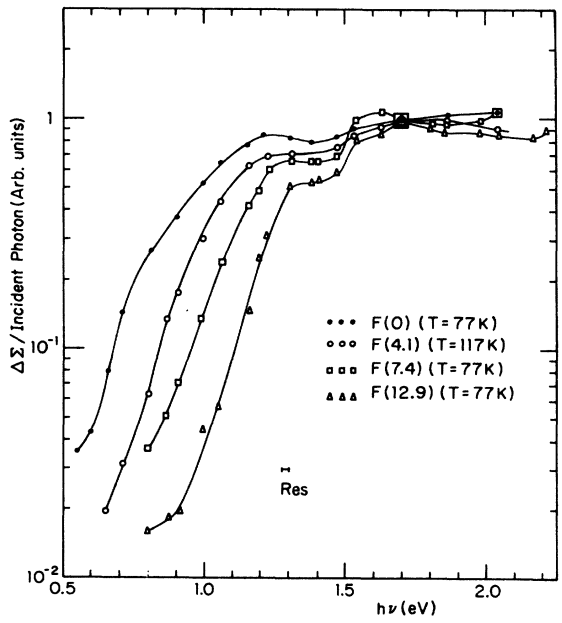

FIG. 2. Photoconductance vs photon energy for the same films as in Fig. 1. (The photoconductance was measured at the indicated temperatures).

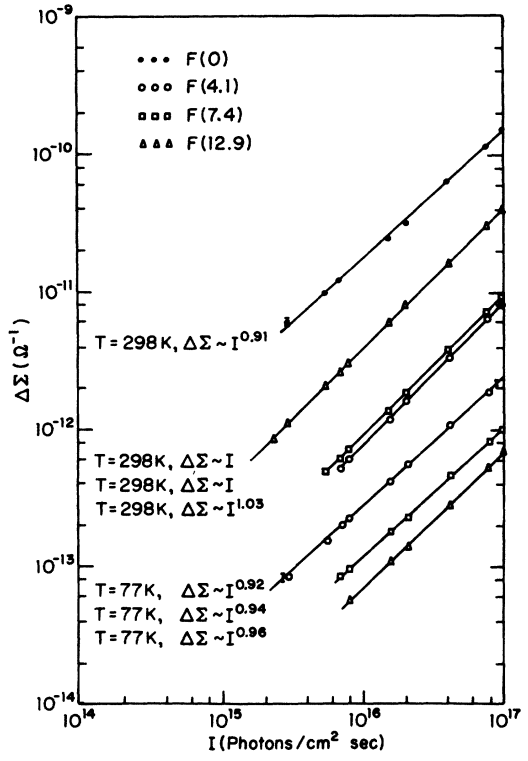

FIG. 3. Photoconductance of the same films at the indicated temperatures, measured at $h\nu = 1.96$ eV, vs light intensity.

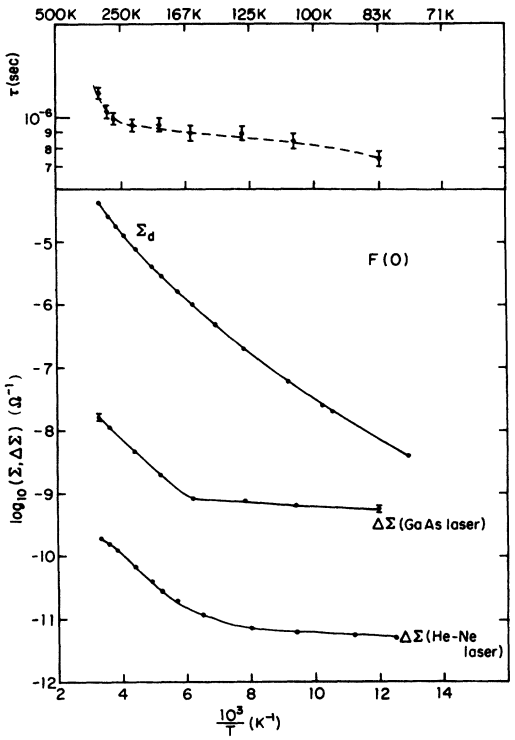

FIG. 4. *Lower scale*: Dark conductance and photoconductance of the film $F(0)$ vs reciprocal temperature. The photoconductance was measured with an He-Ne and a GaAs laser with photon fluxes 1.0×10^{17} photons/cm^{2}sec and 3.0×10^{19} photons/cm^2 sec, respectively. *Upper scale*: The response time of the same film, as determined with the GaAs laser, vs reciprocal temperature.

0.96. The nonhydrogenated sample $F(0)$ was measured only at room temperature, and the photoconductivity was found to depend sublinearly on light intensity with a power of 0.91. A similar trend of light-intensity dependence has been reported by Fischer and Vornholz[12] on evaporated amorphous Ge, using the same photon energy but much higher light intensity. At high temperatures, they found a linear dependence on light intensity, while at low temperatures they found a sublinear dependence with a power of about 0.8.

According to Fig. 3 the magnitude of the photoresponses at 298 and 77 K depend differently on hydrogenation. At 298 K, the photoresponse increases with the degree of hydrogenation, while at 77 K, it decreases. The room-temperature photoresponse of the *unhydrogenated* film does not follow this pattern, and we shall discuss this difference later.

3. Temperature dependence

The temperature dependence of the photoconductance was measured with two different light sources: the He-Ne laser ($h\nu = 1.96$ eV; modulation frequency: 600 Hz; photon flux: 1.0×10^{17} photons/cm^2 sec) and the GaAs laser ($h\nu = 1.47$ eV, pulse duration: 3 μsec, photon flux $= 3.0\times10^{19}$ photons/cm^2 sec). The dark conductance Σ and the change in conductance $\Delta\Sigma$ on illumination with the above sources is illustrated in Figs. 4–7 for the four types of samples. For each sample the $\Delta\Sigma$ curves, which were measured with the two light sources, have qualitatively similar temperature dependencies. At higher temperatures, the photoconductance appears to be thermally activated. At some temperature, which for the different types of samples varies between 130 and 250 K, the activation energy decreases significantly, and the photoconductance becomes only weakly temperature dependent. Besides this general trend one can identify some particular characteristics in the $\Delta\Sigma$ curves of the four types of samples.

For the sample $F(0)$ (see Fig. 4), the change in the temperature dependence of $\Delta\Sigma$ occurs at approximately 170 K. At higher temperatures $\Delta\Sigma$ has an activation energy of approximately 0.1 eV, while at lower temperatures the curve has a slope of approximately 8×10^{-3} eV. A similar temperature dependence for photoconductivity of evaporated a-Ge has recently been reported by Hirose *et al.*[15]

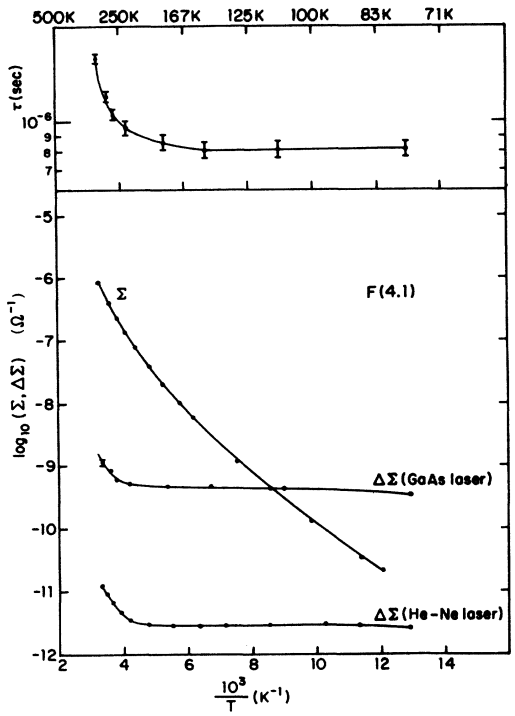

FIG. 5. Same data as in Fig. 4 for sample $F(4.1)$.

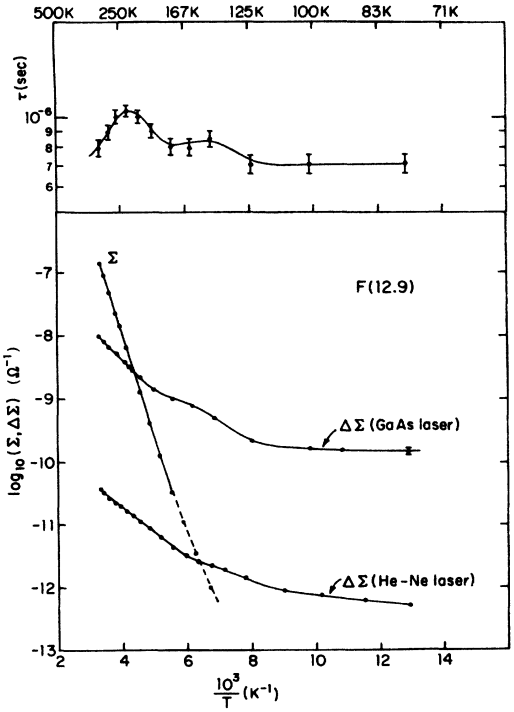

FIG. 7. Same data as in Fig. 4 for sample $F(12.9)$.

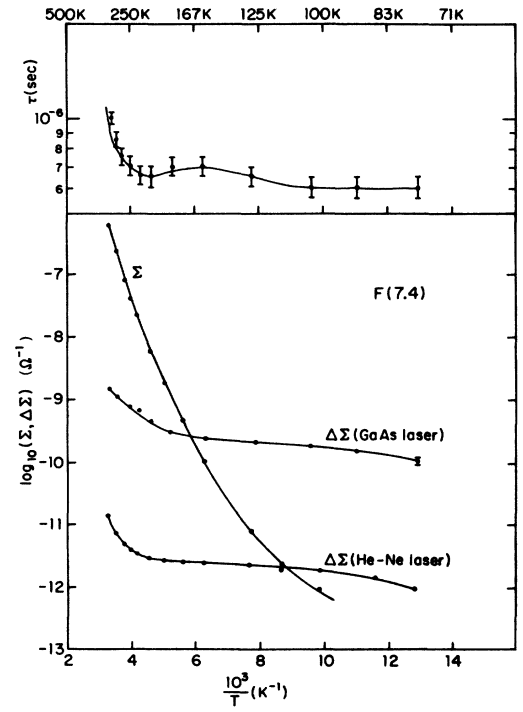

FIG. 6. Same data as in Fig. 4 for sample $F(7.4)$.

They find that above 170 K the photoconductivity has a slope of 0.1 eV, while at lower temperatures the slope decreases to 0.03 eV.

For the sample $F(4.1)$, (see Fig. 5) the change in the temperature dependence of $\Delta\Sigma$ occurs at approximately 225 K. At lower temperatures $\Delta\Sigma$ is nearly temperature independent, changing slope slightly at 100 K.

For the sample $F(7.4)$ (see Fig. 6), the high-temperature mechanism sets in at about 200 K. The tail, which was observed in the previous sample below 100 K, now is more pronounced and starts at higher temperatures.

For the sample $F(12.9)$ (see Fig. 7), $\Delta\Sigma$ has more structure in its temperature dependence. The high-temperature activation energy disappears more gradually as the temperature is lowered.

The photoconductivity at low temperatures was found to decrease with the degree of hydrogenation but not as drastically as the dark conductivity. Thus, for example, at 77 K we have the ratios

$$\Delta\Sigma[F(12.9)]/\Delta\Sigma[F(0)] \simeq 5 ,$$

$$\Sigma[F(12.9)]/\Sigma[F(0)] \gtrsim 10^5 .$$

(The geometrical factor to convert to conductivities is the same within 30% for all samples.)

4. Transient photoconductivity

The photoconductivity kinetics were examined by studying the decay of the photoconductivity after illumination with the GaAs laser. Representative photoconductivity relaxation curves, taken near room temperature for the four types of samples, are shown in Fig. 8. Similar curves were taken at several temperatures down to liquid nitrogen temperature and were found to have approximately the same shapes.

The decay curves for the nonhydrogenated samples $F(0)$ and for the slightly hydrogenated ones $F(4.1)$ can be fitted to exponential curves. However, the shape of the curves changes with the degree of hydrogenation, and for the most hydrogenated films $F(12.9)$, one can clearly detect a fast and a slow component.

The decay times of these curves are approximately a factor of ten longer than the decay time of the laser pulse and the RC time constant of the measuring circuit. The decay time, measured at the $1/e$ point of the relaxation curves, is plotted in the insets of Figs. 4–7 on an expanded logarithmic scale. For the sample $F(12.9)$, in which the slow component is a significant part of the signal, the $1/e$ point was read in the extrapolated part of the fast component.

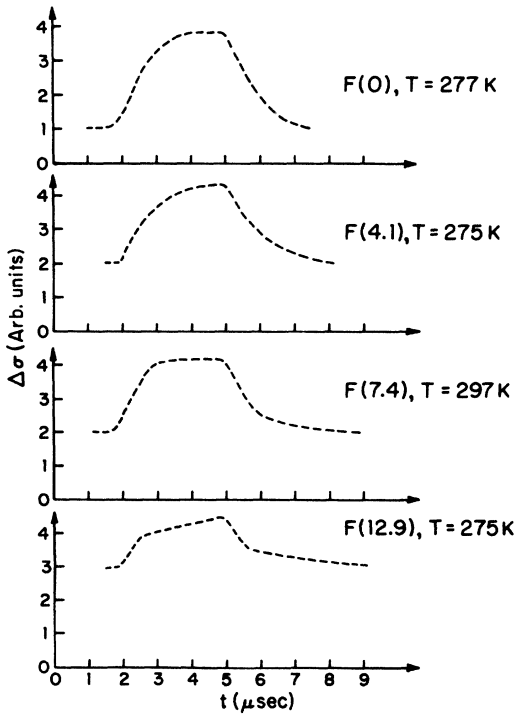

FIG. 8. Photoconductivity relaxation curves taken with the GaAs laser. The shape of the curves changes with the degree of hydrogenation. Applied field $E < 10^3$ V/cm.

By inspection of Figs. 4–7, one finds that for the first three types of samples (see Figs. 4–6) there is a qualitative agreement in the temperature dependence of the decay time and the steady state photoconductance. In other words, both τ and $\Delta\Sigma$ are almost constant at low temperatures, and they both increase at higher temperatures, although with different slopes. For the most hydrogenated sample, $F(12.9)$ (see Fig. 7), τ and $\Delta\Sigma$ have approximately the same qualitative behavior from 77 to 230 K. At higher temperatures τ decreases, although $\Delta\Sigma$ continues to increase.

Decay times of this order (~ 1 μsec) appear to be considerably smaller than have been reported previously for a-Ge. Fischer and Vornholz[12] report an upper limit of 1 msec. Donovan *et al.*[11] report a time constant of approximately 50 msec above 200 K and identify that with the bolometric effect; between 77 and 200 K they find a time constant less than 1 msec. They also report that in the whole temperature range there is a component with a time constant between 1 to 10 μsec. Vescan and Croitoru[14] report a decay time of less than 0.5 sec.

IV. DISCUSSION

A. Conducting states

The investigation of dark transport[5] in this material produced the following conclusions: At high temperatures the majority carriers are electrons that move in the conduction band with a thermally activated mobility of activation energy approximately 0.2 eV. Lewis suggested that this form of the mobility indicates small polaron formation. At low-temperatures transport proceeds through states at the Fermi level.

In this section, we discuss whether the transport of photogenerated carriers involves the same states as for dark carriers, a question on which earlier opinions vary. Fischer and Vornholz[12] suggest that the photocarriers in evaporated a-Ge conduct by hopping close to the equilibrium Fermi level in the temperature range from 77 to 560 K. The justification for this argument is that the density of states within the gap, for evaporated a-Ge, is so high that the photocarriers fall rapidly in a large number of successive steps down to the relatively smaller density of states near the Fermi level, where they conduct for a time, rather than conducting in a high-energy band and then making one (or a very few) recombinative transitions. To account for the observed *positive* photoconductivity, these authors assumed that the density of states at the quasi-Fermi levels is higher than the density at the equilibrium Fermi level. The recombination lifetime in this model is the time which an electron takes to find a hole in the localized states

at the Fermi level. To account for an almost temperature-independent photoconductivity at low temperatures, they postulated that the recombination is diffusion limited. In other words, they assumed that the recombination lifetime is inversely proportional to the total conductivity [$\tau \sim 1/(\sigma + \Delta\sigma)$].

This hypothesis for evaporated Ge can be checked against our transient photoconductivity data. Comparison is best made with the unhydrogenated sample (see Fig. 4), where the model is most likely to be applicable because of the higher density of states in the gap. For this sample the dark conductance was found to be much higher than the photoconductance, for the light sources used in the present experiment (for the thickness of our samples the penetration depth of the employed light source[6] is such that the relative relation of Σ and $\Delta\Sigma$ is similar to that of σ and $\Delta\sigma$), and therefore the recombination lifetime is determined by the relation $\tau \sim 1/\Sigma$. Since Σ decreases by four orders of magnitude between 300 and 77 K, the recombination lifetime should show a corresponding increase. However, τ was found to have a very small temperature dependence, of sign opposite to the predictions of the Fischer-Vornholz model. In addition, the recombination lifetime should strongly depend on the degree of hydrogenation of the sample, since hydrogen reduces the density of states in the pseudogap, where hopping and recombination takes place. In the present experiment, however, τ was found to be almost independent of the degree of hydrogenation (see Figs. 4–7). We conclude that the Fischer-Vornholz model is not applicable to our experimental results.

The alternative model, in which the photocarriers conduct in states away from the Fermi level, in the whole temperature range, has been suggested by Moustakas, Connell, and Paul[13] and by Vescan and Croitoru.[14] However, these authors are forced to postulate specific models for the mobility and lifetime that disagree in their details with our experimental results. Thus, for example, in the model of Moustakas *et al.* the mobility was assumed to be thermally activated over the whole temperature range. Then, in order to explain the observed temperature-independent product $\mu\tau$ at low temperatures, the recombination lifetime was assumed to vary as $1/\mu$. In the present experiments, τ was found to be temperature independent in this temperature range. Vescan and Croitoru assumed that the photocarriers conduct in extended states, but it will be shown in Sec. IV C that the calculated mobility from our results is inconsistent with extended state conduction.

In this paper, we suggest that indeed the photocarriers conduct in states away from the Fermi level, and we use both the transient and the steady-state photoconductivity data to get information regarding their nature. We believe that these states are the same ones where dark conduction occurs at high temperatures. Apparently, because of the recombination mechanism, which may have to do with the density-of-state distribution in the gap, the states near the equilibrium Fermi level do not contribute much to the transport of photocarriers which are initially created high in the conduction band. As a result of the fact that the low-temperature *dark* transport occurs at the equilibrium Fermi level while transport of the *photocarriers* is assumed to occur at states away from the Fermi level, the direct comparison of the experimental Σ and $\Delta\Sigma$ curves of Figs. 4–7 is meaningless. Instead, one should extrapolate the high-temperature thermally activated dark conductance to low temperatures and compare the $\Delta\Sigma$ curves with the extrapolated Σ. In the present work, since the measurements were extended only to 300 K, accurate extrapolation of the thermally activated part of Σ is possible only for the most hydrogenated sample (see Fig. 7). From that, one concludes that the photoconductance $\Delta\Sigma$ produced by the GaAs laser is much greater than the extrapolated high-temperature dark conductance Σ over almost the whole temperature range. Thus, the density of dark carriers n_0 in the states where photoconduction occurs is much smaller than the density of photocarriers Δn.

In Sec. IV B we derive expressions for the transient and steady-state photoconductivity.

B. Expressions for steady-state and transient photoconductivity

In order to discuss the steady-state photoconductivity, the transient-photoconductivity response, and both their temperature dependencies, we shall adopt at first a rather general model of the state density as a function of energy and the movement of carriers between these states. The energy of the incident photon is deemed sufficient to produce at least one carrier initially in an extended state of relatively high mobility (here, this simply means high with respect to the mobility of carriers at any energy in the pseudogap). For simplicity, we shall suppose that one carrier, say the electron, makes the dominant contribution to the transport; but if both electrons and holes contribute, the qualitative effects are much the same. We shall suppose that the electron in an initially high mobility state has three scenarios for recombination with a hole. (a) It may recombine directly with the hole, with photon or phonon (multiphonon) emission. Alternatively, it may recombine via a type of recombination center, where, by postulate,

it has zero mobility. In either of these cases, once it falls from state $|c\rangle$ to state $|r\rangle$ it conducts no more. (b) It may fall into intermediate states of lower mobility $|i\rangle$, and trickle through them with phonon emission until it lands in states of zero mobility, when it has, for all purposes, recombined. (c) It may fall into the intermediate states of lower mobility, whence it may be re-excited back into a high-mobility state, there to make a new choice of future adventures. Calling n_c the number of electrons in conducting states $|c\rangle$, and n_i the average number in the intermediate states $|i\rangle$, we have

$$\frac{dn_c}{dt} = G + A_{ic} n_i - B_{ci} n_c - B_{cr} n_c \ , \tag{1}$$

$$\frac{dn_i}{dt} = B_{ci} n_c - A_{ic} n_i - B_{ir} n_i \ , \tag{2}$$

$$\frac{n_i}{n_c} = R(N_c, N_i, T) \ , \tag{3}$$

$$\Delta\sigma = e(n_c \mu_c + n_i \mu_i) \ . \tag{4}$$

Here G is the generation rate of electron-hole pairs by light (thermal transitions from the recombination centers have been neglected), A_{pq} is the rate of upward transitions from state p to state q, B_{pq} the rate of downward transitions from state p to state q, r is a final recombination state, N_c, N_i are the densities of states $|c\rangle$ and $|i\rangle$, μ_c, μ_i the mobilities in states $|c\rangle$ and $|i\rangle$, and R is the ratio of carrier densities in the states $|i\rangle$ and $|c\rangle$. From Eqs. (1)–(3) we get

$$\frac{d}{dt}(n_c + n_i) = \frac{d}{dt}(n_c + n_c R) = G - B_{cr} n_c - B_{ir} n_c R \ . \tag{5}$$

According to experimental data the number of photocarriers in the states $|c\rangle$ is much higher than the number of dark carriers in the same states. Therefore, Eq. (5) can be integrated subject to the boundary condition $n_c = 0$ at $t = 0$,

$$n_c(t) = [G/(B_{cr} + B_{ir} R)](1 - e^{-t/\tau_0}) \ , \tag{6}$$

$$n_i(t) = R n_c(t) \ , \tag{7}$$

where

$$\tau_0 = (1 + R)/(B_{cr} + B_{ir} R) \tag{8}$$

is the response time of the photoconductor. From Eqs. (4), (6), and (7) the transient and the steady-state photoconductivity can be calculated

$$\Delta\sigma(t) = e n_c(t)(\mu_c + R\mu_i) \ , \tag{9}$$

$$\Delta\sigma(s) = \frac{eG}{B_{cr} + B_{ir} R}(\mu_c + R\mu_i) \ , \tag{10}$$

where (s) represents steady state. According to Eq. (10) the transport in the states $|c\rangle$ dominates at high temperatures both because $\mu_c \gg \mu_i$ and because R is small. However, at low temperatures the product $R\mu_i$ may become comparable to or larger than μ_c and the transport through the intermediate states $|i\rangle$ will be the dominant one. In any case, the drift mobility is

$$\mu_D = (\mu_c + R\mu_i)/(1 + R) \ . \tag{11}$$

By combining Eqs. (8), (10), and (11), we get

$$\Delta\sigma(s) = eG\mu_D \tau_0 \ . \tag{12}$$

Special cases

(i) Suppose that the intermediate states play no role in the transport and recombination. Then the quantities A_{ic}, B_{ci}, B_{ir}, R, and μ_i are zero. In this case, the response time $\tau_0 = 1/B_{cr}$ is the recombination lifetime τ of electrons. The temperature dependence of τ, if any, will depend on the recombination mechanism. Also, the drift mobility is the microscopic mobility μ_c in the states $|c\rangle$. Then

$$\Delta\sigma(t) = eG\mu_c \tau(1 - e^{-t/\tau}) \ , \tag{13}$$

$$\Delta\sigma(s) = eG\mu_c \tau \ . \tag{14}$$

(ii) Suppose there is no probability of direct recombination from the conduction states, i.e., $B_{cr} \approx 0$. Then

$$\tau_0 = (1 + R)/B_{ir} R \ , \tag{15}$$

$$\Delta\sigma(t) = (eG/B_{ir} R)(\mu_c + R\mu_i)(1 - e^{-t/\tau_0}) \ , \tag{16}$$

$$\Delta\sigma(s) = (eG/B_{ir} R)(\mu_c + R\mu_i) \tag{17}$$

(iii) Suppose there is no probability of direct recombination out of the intermediate states, but only via the conduction band, i.e., $B_{ir} = 0$. Then

$$\tau_0 = (1 + R)/B_{cr} \ , \tag{18}$$

$$\Delta\sigma(t) = (eG/B_{cr})(\mu_c + R\mu_i)(1 - e^{-t/\tau_0}) \ , \tag{19}$$

$$\Delta\sigma(s) = (eG/B_{cr})(\mu_c + R\mu_i) \ . \tag{20}$$

In order to examine these cases and their relevance to the experimental results, one should take into account that the parameters B have little or no temperature dependence, whereas A and R are exponentially dependent on T. In order to write an explicit form for R, we assume that the intermediate states $|i\rangle$ have an average energy E_i more than a few kT above the equilibrium Fermi level, so that

$$R = (N_i/N_c) \exp(E_c - E_i/kT) \ . \tag{21}$$

Case (i) suggests that the temperature dependence of τ_0 depends on the specific recombination mechanism. Case (ii) suggests that τ_0 varies with

T as $(1+R^{-1})$. This implies that τ_0 increases as T increases, which fits the high-temperature, but not the low-temperature data. Case (iii) suggests that τ_0 can only decrease as T increases, reflecting the behavior of R. This could be the cause of the high-T decrease for sample F (12.9), but it is clear that the other samples display exactly the opposite behavior.

Although the foregoing remarks seem to provide a basis for choice of the principal mechanism of recombination, we choose to proceed with the analysis of the results using the general Eq. (12).

C. Determination of the mobility

The steady-state photoconductance, derivable from Eq. (12), may be rewritten[21]

$$\Delta\Sigma(s) = (h/l)\eta e(1-S)I(1-e^{-\alpha d})\mu_D\tau_0 , \qquad (22)$$

where d is the thickness and h is the width of the sample, l is the distance between the electrodes, η is the quantum efficiency, e is the electronic charge, S is the front surface reflectance, I is the incident-light intensity (photons/cm^2 sec), and α is the absorption coefficient. For the radiations of the He-Ne laser ($h\nu = 1.96$) and GaAs laser ($h\nu = 1.47$ eV), the quantum efficiency can be considered equal to one. Also for these energies the absorption coefficient for all samples investigated is larger than 10^5 cm^{-1}.[6] Since the thickness of the samples is approximately $d \sim 10^{-4}$ cm, the term $1-e^{-\alpha d}$ can be approximated by one.

Equation (22) predicts that the photoconductance depends linearly on light intensity. Figure 3, however, shows that under some conditions, particularly low temperatures, the photoconductance has a small sublinear behavior on light intensity (exponent between 0.92 and 0.96). This sublinearity may arise from the experimental conditions for the following reasons. The light is not absorbed uniformly throughout the sample but attenuates rapidly below the illuminated surface. Thus, depending on the ratio of the densities of dark and photocarriers in the states where conduction occurs, it may happen that recombination near the surface is bimolecular while that in the bulk is monomolecular. Such a combination has been invoked by Tabak and Warter[22] to interpret photoconductivity results on cadmium sulfide and by Spear *et al.*[23] to account for results on a-Si. In our case, the observed sublinear behavior could be attributed to 10% and 15% of the carriers suffering bimolecular recombination.

The drift mobility can be calculated from Eq. (22) using the $\Delta\Sigma$ and τ_0 values of Figs. 4–7 and the light intensity of the corresponding laser. [The (10 to 15)% correction in the $\Delta\Sigma$ values is neglected to a first approximation.] The mobility for the four types of sample as a function of temperature is illustrated in Fig. 9. By inspection of this figure one can reach some very important conclusions about the mobility in this material. At high temperatures the mobility is thermally activated with a typical activation energy of 0.1 eV. At low temperatures the activation energy decreases significantly. The temperature at which the mobility changes character varies for the different types of sample between 130 and 250 K. This critical temperature is displaced to lower values with hydrogenation. The variations in the photoconductances with hydrogenation, discussed with reference to Fig. 3, are now seen to be related to changes in the drift mobilities. The critical temperature for the unhydrogenated sample $F(0)$ occurs at approximately 170 K and does not follow the trend of the hydrogenated films. For sample $F(0)$, the thermoelectric power is positive at high temperature,[24] and by inference the dominant photocarriers may be holes. We speculate that this could be the reason why the temperature dependence of its μ_D in Fig. 9 is different from that of the hydrogenated films.

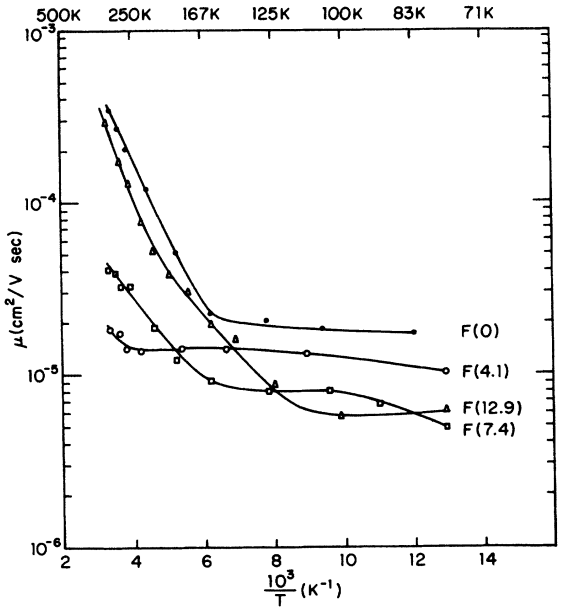

FIG. 9. Drift mobility of the investigated films vs reciprocal temperature. The results were calculated using the steady-state and transient photoconductivity data taken with the GaAs laser.

The absolute value of the room-temperature mobility varies between 3×10^{-4} cm^2/V sec and 2×10^{-5} cm^2/V sec for the different types of sample. The low-temperature mobility has an average value of approximately 1×10^{-5} cm^2/V sec. (Direct measurements of the drift mobility in this material

have not been reported in the literature. However, Hall mobilities, whose comparability with the present estimates is doubtful, have been reported for evaporated a-Ge by Seager *et al.*[25] These authors find a thermally activated mobility at temperatures above 300 K with an absolute value at room temperature of 10^{-3} cm^2/V sec.)

D. Proposed models

1. Transport mechanisms

A satisfactory model must account for the temperature dependence of the drift mobility of Fig. 9. This drift mobility may be the intrinsic mobility of carriers which transport in a group of states of nearly the same energy and wavefunction (the so-called microscopic mobility) or it may be influenced by occasional trapping in other states where the carriers have much lower mobility.

We shall consider the second possibility first. Equation (11), which is applicable, gives for the mobility in the high- and low-temperature limits

$$\mu_D(T_h) = \mu_c/(1+R)\ , \tag{23}$$

$$\mu_D(T_l) = \mu_i R/(1+R)\ , \tag{24}$$

where T_h and T_l are high and low T, respectively.

If we then plausibly assume that R is much larger than one, Eqs. (23) and (24) become

$$\mu_D(T_h) \to \mu_c \frac{N_c}{N_i} \exp\left(\frac{-(E_c - E_i)}{kT}\right), \tag{25}$$

$$\mu_D(T_l) \to \mu_i\ . \tag{26}$$

Applying Eq. (25) to the high-temperature part of Fig. 9 and assuming the T dependence of μ_c to be much weaker than exponential, we obtain $E_c - E_i = 0.1$ eV and $\mu_c N_c/N_i = \frac{1}{60}$. Thus, this approach implies an average trap depth which is not unreasonable. Suppose, however, we assume that the conducting states $|c\rangle$ are the extended states, and further assume μ_c determinable by calculation on the random phase approximation[26]

$$\mu_c = \pi e a^5 Z J^2 N_c/\hbar k T\ . \tag{27}$$

The values to be inserted into (27) for a, J, and N_c are doubtful, but, if we choose the following usual and perhaps plausible set—a: scattering distance, 2.5 Å; Z: coordination number, 4; J: hopping integral, 1 eV; T: 300 K; and N_c: state density, 10^{21} eV^{-1} cm^{-3}—we obtain $\mu_c \sim 7$ cm^2/V sec and $N_i/N_c = 400$. This value for N_i/N_c is physically implausible. If J or N_c is reduced to make $\mu_c \sim 10^{-2}$ cm^2/V sec (the lowest estimate we have found in the literature), then N_i/N_c becomes approximately 0.6, which is perhaps acceptable. Again, if the mobility μ_c is smaller than that appropriate to extended states and calculable on the basis of Eq. (27), and instead is some hopping transport with a weak T dependence, then acceptable values of N_i/N_c will be found. Of course, assessment of an overall preference for a model of transport should take into account what can be learned from the T dependence of τ (Sec. IV D 2).

From Eq. (26), the low-temperature mobility should be that of electrons hopping among localized states,[27] or $\ln\mu_D \propto T^{-1/4}$. The experimental results fit this T dependence satisfactorily, but this should not be taken as proof of this relationship, since other weak T dependencies might suit as well.

Next, we consider the possibility that the μ_D of Fig. 9 is the microscopic mobility, and try to infer the transport mechanism from its magnitude and T dependence. Clearly the magnitude and T dependence are inconsistent both with conventional quasifree particle motion with occasional scattering, and with diffusive transport of the type described by Eq. (27). However, the curve of Fig. 9 shows a remarkable similarity to the theoretical predictions for the mobility of small polarons.[7-10] We recall that we argued in Sec. IV A that the transport mechanism was the same for photoproduced carriers and dark carriers at high temperatures; in this respect it is notable that Lewis concluded,[5] from his extensive analysis of dark-transport measurements in this laboratory, that the polaron mechanism was the favored candidate.

In an ideal crystal, the small polaron moves by hopping at high temperatures with an activation energy of half the polaron binding energy, W_p. At low temperatures, it moves without thermal activation like a very-heavy-mass band electron. The temperature ranges where transition between the two kinds of transport occurs depend on the details of the coupling of the electron to both the optical and the acoustic phonons, and thus is model dependent. Friedman[10] puts this critical temperature between $\frac{1}{4}\Theta$ and $\frac{1}{2}\Theta$, where Θ is the characteristic temperature of the optical phonons, $\hbar\omega_0/k$. For a disordered system of disorder energy W_d, the high-temperature activation energy for hopping becomes $\frac{1}{2}(W_p + W_d)$, and an activation energy of W_d is introduced for the low temperature mobility. For a-Ge, $\Theta \approx 400$ K, indicating a transition region between 100 and 200 K, which clearly agrees with the T dependence of μ_D in Fig. 9. If this interpretation is correct, then $W_d \approx 0.01$ eV and $W_p \approx 0.2$ eV. We may also evaluate the significance of the magnitude of μ_D by writing it as $\mu_D = \mu_0 e^{-0.1/kT}$. Then μ_0 may be determined as 1.5×10^{-2} cm^2/V sec, for the sample F (12.9) and this value compared with the mobility $\mu_{0,\mathrm{dark}}$ of the dark carriers. The latter quantity may be estimated from the data of Fig. 1 for sample F (12.9), for which the dark conductivity is clearly thermally activated over an extended high-temperature

range. We can write

$$\sigma = \sigma_0 e^{-E_a/kT} = Ne\mu_0 e^{-E_a/kT} = 30\ e^{-E_a/kT}\ , \qquad (28)$$

where N is the number of equivalent hopping sites for a small polaron.[27] Following Emin *et al.*,[28] we assume that each atomic site can be a hopping site for a small polaron. Thus $N = 4 \times 10^{22}$ cm^{-3} and $\mu_{0,\,\mathrm{dark}} = 5 \times 10^{-3}$ cm^2/V sec. Thus, there is reasonably satisfactory agreement between the two estimates of μ_0, and support both for the postulated identity of phototransport and high-temperature dark transport, and with the hypothesis of a small polaron mechanism.

2. *Recombination mechanism*

The very weak dependences of τ_0 on temperature below 200 K and on hydrogenation are very important in our consideration of the mechanism of recombination. We shall argue that none of the four suggested ways in which hydrogenation might affect τ_0, μ_D and $\Delta\sigma$(steady-state), viz., (a) reduction of density of recombination centers by compensation of dangling bonds; (b) increased probability of multiphonon recombination by introduction of high energy localized vibrational modes; (c) increased lifetime and reduced mobility for carriers actually near the Fermi level in the pseudogap, by reduction of the state density there; and (d) possible introduction of Ge-H antibonding states near the bottom of the conduction band, have been confirmed, and that, unless there exist fortuitous cancellation effects, a qualitatively different mechanism of recombination (and transport) of photocarriers is required.

We first argue that the dangling-bond states which are compensatable by hydrogen are the most important of the conventional recombination centers in the pseudogap. It is clear that such states (or paired states reconstructed from them) must dominate the state density at E_F, since the compensation by hydrogen dramatically reduces the low-temperature transport. For a second independent set of centers to dominate the recombination, they must have a greater capture cross section for electrons and/or holes. However, since the dangling bond or reconstructed states very probably are present as neutral and positively and negatively charged centers, it is very unlikely that this is the case. Therefore, since τ_0 is essentially unaffected by hydrogenation, recombination via conventional centers is not the dominant vehicle.

It might be argued, in principle, that the first effect, a reduction in density of recombination centers, may be offset by the second, an increase in multiphonon recombination. The near cancellation that occurs for all levels of hydrogenation makes this unlikely.

The third possibility applies only in the case of the Fischer-Vornholz model,[12] which we already argued in Sec. IV did not apply to our data.

It seems unlikely that the fourth possibility, Ge-H antibonding states near the bottom of the conduction band, occurs for our samples. If it did, we would expect a decrease in τ_0, through the mechanism (b) above, and probably also a decrease in μ_D.

We propose a different model, to wit, that the photocarriers form small polarons out of the band states and that these polarons degrade in energy by phonon emission, all the while transporting current by moving in the applied field, until their contribution to $\Delta\sigma$ is no longer significant. At the lower temperatures, the polaron formed out of intrinsic states gradually changes into a polaron formed out of defect pseudogap states, without scattering abruptly into states of appreciably lower energy. Thus, the density of pseudogap states, which may be affected by hydrogenation, has only a weak effect on the time for the polaron to degrade. At the higher temperatures, there exists the possibility that the polaron may gain energy from the lattice, depending on the ratio of kT to its binding energy. We suggest that this is the reason for the high-temperature increase in τ_0, observed in all samples at about the same temperature. In the most-hydrogenated sample *F* (12.9) the τ_0 decreases again at the very highest temperature and the detailed shape of the relaxation curves of Fig. 8 changes. For this we suggest the tentative explanation that it indicates a different mechanism of recombination, perhaps caused by the high density of Ge-H antibonding states which the excited polarons then encounter.

It is to be noted that the proposed mechanisms of recombination and transport are self-consistent. The polaron, transforming itself as it transports from a band electron with phonon cloud into an electron in a state in the pseudogap with a different lattice distortion, is insulated to a major extent from the effects of temperature and pseudogap state density reduction by hydrogenation. However, both τ_0 and μ_D increase at temperatures sufficient to re-excite the polaron into a higher energy state, or to ionize it.

ACKNOWLEDGMENTS

The authors wish to thank G. A. N. Connell, A. J. Lewis, and D. A. Anderson for many suggestions and discussions. We also thank M. A. Paesler and J. R. Pawlik for critical comments on the manuscript. The technical assistance of R. Centamore, D. MacLeod, and L. DeFeo is appreciated.

*Work supported by NSF Grant No. DMR-76-15325.

†Present address: Exxon Research and Engineering Co., Linden, N. J., 07036.

[1]W. Paul, Thin Solid Films 33, 381 (1976).
[2]R. J. Temkin, W. Paul, and G. A. N. Connell, Adv. Phys. 22, 581 (1973).
[3]M. H. Brodsky, R. S. Title, K. Weiser, and G. D. Pettit, Phys. Rev. B 1, 2632 (1970).
[4]W. Paul, G. A. N. Connell, and R. J. Temkin, Adv. Phys. 22, 529 (1973).
[5]A. J. Lewis, Phys. Rev. B 14, 658 (1976).
[6]G. A. N. Connell, and J. R. Pawlik, Phys. Rev. B 13, 787 (1976).
[7]David Emin, Adv. Phys. 24, 305 (1975).
[8]David Emin, in *Linear and Nonlinear Electron Transport in Solids*, edited by J. T. Devreese and V. E. Van Doren (Plenum, New York, 1976).
[9]J. Schnakenberg, Phys. Status Solidi 28, 623 (1968).
[10]L. Friedman, Phys. Rev. 135, A233 (1964).
[11]T. M. Donovan, M. L. Knotek, and J. E. Fisher, in *Proceedings of the Fifth International Conference on Amorphous and Liquid Semiconductors*, edited by J. Stuke and W. Brenig, (Taylor and Francis, London, 1974), p. 549.
[12]R. Fischer and D. Vornholz, Phys. Status Solidi B 68, 561 (1975).
[13]T. D. Moustakas, G. A. N. Connell, and W. Paul, in *Electronic Phenomena in Non-Crystalline Semiconductors*, edited by B. T. Kolomiets (Academy of Sciences of the USSR, 1976), p. 310.
[14]L. Vescan and N. Croitoru, in Ref. 13, p. 244.
[15]M. Hirose, I. Ohe, and Y. Osaka, in Ref. 13, p. 255.
[16]J. E. Rowe, Solid State Commun. 17, 673 (1975).
[17]K. C. Pandey, Phys. Rev. B 14, 1557 (1976).
[18]This conclusion is based on the fact that the conductivity measured by the four-probe method is identical to the measured by the two-probe method.
[19]A. J. Lewis, G. A. N. Connell, W. Paul, J. R. Pawlik, and R. J. Temkin, *Tetrahedrally Bonded Amorphous Semiconductors*, edited by M. H. Brodsky, S. Kirkpatrick, and D. Weaire (AIP, New York, 1974), p. 27.
[20]T. D. Moustakas and G. A. N. Connell, J. Appl. Phys. 47, 1322 (1976).
[21]S. M. Ryvkin, *Photoelectric Effects in Semiconductors*, translated by A. Tybulewicz (Consultants Bureau, New York, 1964).
[22]M. D. Tabak and P. J. Warter, Phys. Rev. 148, 982 (1966).
[23]W. E. Spear, R. J. Loveland, and A. Al-Sharbaty, J. Non-Cryst. Solids 15, 410 (1974).
[24]A. J. Lewis, Phys. Rev. B 13, 2565 (1976).
[25]C. H. Seager and M. L. Knotek, in Ref. 11, p. 1133.
[26]L. Friedman, J. Non-Cryst. Solids 6, 329 (1971).
[27]N. F. Mott, Philos. Mag. 19, 835 (1969).
[28]David Emin, C. H. Seager, and R. K. Quinn, Phys. Rev. Lett. 28, 813 (1972).